Available online at www.sciencedirect.com
ScienceDirect
Geochimica et Cosmochimica Acta 72 (2009) 1295–1311
Geochimica et Cosmochimica Acta
www.elsevier.com/locate/gca

Experimental tests of the effects of Al substitution on the goethite–water D/H fractionation factor

Weimin Feng *, Crayton J. Yapp

Department of Geological Sciences, Southern Methodist University, 3225 Daniel Avenue, Dallas, TX 75275-0395, USA

Received 16 April 2007; accepted in revised form 17 December 2007; available online 25 December 2007

Abstract

Twelve goethite samples with different degrees of substitution of Al for Fe were synthesized at 22–48 °C and pH values of 1.5–14 under closed system conditions and used to study the effects of Al substitution on the hydrogen isotopic fractionation between goethite and its ambient water. The syntheses followed two pathways: (1) Fe^{3+} hydrolysis in high pH aqueous solutions; (2) oxidation of Fe^{2+} to Fe^{3+} in mid to low pH solutions. XRD and SEM analyses indicated that, irrespective of temperature and pH, goethite was the predominant product of the syntheses in all of the experiments (with degrees of Al substitution as high as ~13 mol %). "High temperature nonstoichiometric" (HTN) water is present in all of the samples and rapidly exchanges D/H with ambient vapor at room temperature. Uncertainties in the value of the apparent D/H fractionation factor (α_{e-v}) between HTN water and ambient exchange water at 22 °C lead to significant uncertainties in determinations of the δD values of structural hydrogen (δD_s) in goethites which contain high proportions of HTN water. As determined for the samples of this study, α_{e-v} has a nominal value of 0.942 (±0.02). δD_s values determined using an α_{e-v} value of 0.942 indicate that Al substitution increases the δD value of structural hydrogen in goethite by about 1.4 (±0.4)‰ for each increase in Al of 1 mol %. This dependence on Al is of the same sign as, but somewhat larger in magnitude than, the effect of Al predicted by a published model (~0.7‰ per mol % Al). The overall uncertainties in the current results suggest that an increase of ~1‰ per mol % Al, as adopted by previous studies, may be a reasonable estimate with which to adjust δD_s values of natural goethites to those of the pure FeOOH endmember and could be valid for degrees of Al substitution of up to at least 15 mol %. These synthesis experiments also yield a hydrogen isotopic fractionation factor ($^{D}\alpha_{G-W}$) between pure goethite (α-FeOOH) and liquid water of 0.900 (±0.006), which is analytically indistinguishable from the published value of 0.905 (±0.004). Thus, use of an $^{D}\alpha_{G-W}$ value of 0.905 in applications to the FeOOH component of natural goethites is supported by the current study.

1. INTRODUCTION

Goethite (α-FeOOH) is a common mineral formed in oxidizing, wet, surface and near surface environments such as soils; ironstones; bog deposits; spring deposits; gossans; ferromanganese nodules; deposits from acidic streams; oxidized chemical sediments associated with oceanic spreading centers, etc. (Yapp, 2001a). It is found in both young and ancient systems. In the absence of dissolution and reprecipitation, goethite can preserve its stable isotopic composition for times as long as hundreds of millions of years (Yapp, 1991, 1998; Yapp and Poths, 1993; Girard et al., 1997, 2000, 2002). Stable isotope data from goethite have been used to determine: (1) ancient atmospheric P_{CO_2} from the $\delta^{13}C$ and concentration of CO_2 occluded in the structure of the goethite (Yapp, 1987a, 2001b, 2004; Yapp and Poths, 1992, 1993; Tabor et al., 2004a); (2) paleotemperatures and isotopic compositions of waters from the oxygen isotopic compositions of goethite (or hematite) and various co-existing, oxygen-bearing minerals (e.g., Yapp, 1993, 1998; Tabor, 2007); and/or (3) paleotemperatures and isotopic compositions of waters from the combination of oxygen

* Corresponding author.
E-mail address: wfeng@smu.edu (W. Feng).

0016-7037/$ - see front matter © 2007 Elsevier Ltd. All rights reserved.
doi:10.1016/j.gca.2007.12.013

and hydrogen isotopic compositions of a single mineral of goethite (e.g., Yapp, 1987b, 1993, 2000; Girard et al., 2000; Tabor et al., 2004b; Tabor and Yapp, 2005; Hren et al., 2006).

Yapp (1987b, 2000) used the following equation (adapted from Savin and Epstein, 1970) for the relationship between the hydrogen and oxygen isotopic composition of goethite formed in water-dominated systems whose waters are characterized by the isotopic meteoric water line of Craig (1961):

$$\delta D_G = 8\left(\frac{^{D}\alpha_{G-W}}{^{18}\alpha_{G-W}}\right)\delta^{18}O_G + 1000\left[8\left(\frac{^{D}\alpha_{G-W}}{^{18}\alpha_{G-W}}\right) - 1\right] - 6990\,^{D}\alpha_{G-W} \quad (1)$$

In Eq. (1), δD_G and $\delta^{18}O_G$ are measured values for goethite. $^{D}\alpha_{G-W}$ is the hydrogen isotopic fractionation factor between α-FeOOH and water. For pure goethite, $^{D}\alpha_{G-W}$ has an essentially constant value in the range of temperatures characteristic of natural goethite formation (Yapp, 1987b). $^{18}\alpha_{G-W}$ is the oxygen isotopic fractionation factor between α-FeOOH and water and is a function of the temperature of formation (e.g., Yapp, 1990, 2007). Thus, if applicable to the conditions of goethite formation, Eq. (1) can be used to determine paleotemperatures and isotopic compositions of waters.

To actually use measured hydrogen and oxygen isotope ratios (δD_G and $\delta^{18}O_G$) of goethite in Eq. (1) to interpret paleoclimatological information (such as formation temperature), the oxygen and hydrogen isotopic fractionation factors between goethite and its ambient water, $^{18}\alpha_{G-W}$ and $^{D}\alpha_{G-W}$, must be known with confidence. Previous studies have estimated the relationships between goethite–water isotopic fractionation factors and temperature using semi-empirical calculations or synthesis experiments (Yapp, 1987b, 1990, 2007; Müller, 1995; Zheng, 1998; Bao and Koch, 1999; Xu et al., 2002). These studies were focused on the oxygen/hydrogen isotopic fractionation between chemically pure goethite and water. However, in natural systems, other cations commonly substitute for structural iron in goethite (Cornell and Schwertmann, 2003). Among the many cations (e.g., Al, Mn, V, Cr, etc., Cornell and Schwertmann, 2003) that can substitute for Fe in the structure of goethite, Al is the most prominent because of the abundance of Al in the environments of goethite formation and its mobilization with Fe during weathering. In natural systems, Al substitution for Fe is found in goethites from soils, oolitic iron ores, and bauxites (e.g., Norrish and Taylor, 1961; Davey et al., 1975; Mendelovici et al., 1979) and the magnitude of Al substitution can reach 33 mol %. Previous studies indicate that the Al substitution has significant impacts on the physical and chemical properties of goethite, such as crystal unit cell dimensions, the formation rate of the mineral, structural defects, solubility, surface adsorption, dehydroxylation temperature and stretching and OH bending frequencies (Schulze, 1984; Schulze and Schwertmann, 1984; Schwertmann, 1984; Schwertmann et al., 2000a).

Yapp (1993) evaluated the possible effects of Al substitution on goethite–water D/H and $^{18}O/^{16}O$ fractionation through a two end-member solid solution mixing model. For hydrogen isotopes, this effect is indicated by Eq. (2), in which, $^{D}\alpha_{G-W}$, $^{D}\alpha_{Al}$, $^{D}\alpha_{Fe}$, are the hydrogen isotopic fractionation factors between Al substituted goethite and water, the pure Al isomorph of goethite (diaspore, α-AlOOH) and water, and pure goethite (α-FeOOH) and water, respectively. X_{Al} is the mole fraction of Al in the goethite structure, i.e., $[n_{Al}/(n_{Al} + n_{Fe})]$.

$$1000\ln{}^{D}\alpha_{G-W} = 1000\left[\ln{}^{D}\alpha_{Al} - \ln{}^{D}\alpha_{Fe}\right]X_{Al} + 1000\ln{}^{D}\alpha_{Fe} \quad (2)$$

While the thermodynamic mixing model has achieved apparent success in interpretations of data from natural goethites (Yapp, 1997; Girard et al., 2000), the impacts of Al substitution on the isotopic fractionation factor have not been experimentally tested. Moreover, Yapp (1993) noted two limitations in applying the model: (1) because of a lack of data on diaspore (α-AlOOH)-water isotopic fractionation, the model calculations employed data for boehmite (γ-AlOOH), which is not an isomorph of goethite (Cornell and Schwertmann, 2003); (2) the model is based on an assumption of ideal solid solution behavior, but the maximum observed Al substitution of 33 mol % suggests that the solution is non-ideal (e.g., Powell, 1978). In this study, we performed mineral synthesis experiments to determine the magnitude of the effects of Al substitution on the hydrogen isotopic fractionation factor between goethite structural hydrogen and ambient water. The possibility that goethite–water hydrogen isotope fractionation factors determined from mineral synthesis may not correspond to equilibrium values is also discussed.

2. EXPERIMENTAL METHODS

2.1. Synthesis of goethite

Open system syntheses of goethite have commonly been employed to achieve varying degrees of substitution of Al for Fe (e.g., Lewis and Schwertmann, 1979; Goodman and Lewis, 1981; Glasauer et al., 1999; Schwertmann et al., 2000a,b). However, for studies of mineral–water isotopic fractionation, it is simplest if the water-dominated system remains closed throughout the process. For closed system conditions during goethite synthesis, some system variables may change significantly. For example, pH would tend to decrease as the synthesis reaction proceeds because of the consumption of OH^- in the solution.

In this study, we adopted two different methods to synthesize goethite: (method A) Fe^{3+} hydrolysis from soluble Fe^{3+} reagent in high pH aqueous solutions; and (method B) Fe^{2+} oxidation to Fe^{3+} followed by Fe^{3+} hydrolysis in mid to low pH aqueous solutions. In method A, ferrihydrite was the initial precipitate from the solution. With "aging" of the system, the ferrihydrite dissolved with subsequent precipitation of goethite (Cornell and Schwertmann, 2003). This method generally produces well-crystallized acicular goethites. However, published results indicate that goethites formed by this method at 70 °C do not have more than 16 mol % of Al substituted for Fe $[n_{Al}/(n_{Al} + n_{Fe}) \times 100\%]$ even if Al/(Al + Fe) in the initial solution is greater than 33% (Schulze and Schwertmann, 1987). This is because at high concentrations of OH^-, the solubility of Al hydroxides increases, such that Al^{3+} tends to stay

in solution rather than be incorporated into the goethite structure.

On the other hand, goethite synthesized by method B can have Al substitution up to 33 mol % (Schulze and Schwertmann, 1987), but the products are usually poorly crystallized. The processes operating to produce goethite in this method are: (1) the oxidation of Fe^{2+}; (2) the formation of ferrihydrites; and (3) dissolution of these ferrihydrites and subsequent precipitation of goethite.

Synthesis methods can have many outcomes, because many factors determine the final products. Although goethite and hematite are the two thermodynamically most stable phases of iron (III) oxide/hydroxides under oxic conditions (Cornell and Schwertmann, 2003), lepidocrocite (γ-FeOOH), akaganeite (β-FeOOH), ferrihydrite (general formula $Fe_5HO_8{\cdot}4H_2O$) and siderite ($FeCO_3$) can also form in synthesis experiments depending upon the combination of certain factors (Cornell and Schwertmann, 2003). These factors include: (1) pH; (2) different associated aqueous cations and anions; (3) experimental temperature; and (4) oxidation rate (e.g., Lewis and Schwertmann, 1979; Cornell and Giovanoli, 1985; Cornell et al., 1987; Schwertmann et al., 2000a). Except for temperature, these internal variables could not be externally controlled in the closed system syntheses of this study.

In the stable isotope laboratory at Southern Methodist University (SMU), four groups of syntheses were conducted. Each group included from two to four parallel experiments. The differences among groups are largely expressed in terms of temperature, initial pH and/or initial oxidation state of Fe (Table 1). Within a particular group, differences among parallel experiments are manifested primarily in different ratios of $Al^{3+}/(Al^{3+} + Fe^{3+\text{ or }2+})$ in the initial solutions (Table 1). Differences in the proportions of Al and Fe in the initial solutions were intended to yield varying proportion of Al in synthesized goethite to evaluate the effects of Al substitution on goethite–water D/H fractionation factors.

2.1.1. Syntheses by method A: groups 1 and 2

Group 1: In each of three 1000 ml thick-walled, high-density polyethylene bottles (labeled as SFO-1-1, SFO-1-2 and SFO-1-4, Table 1), ~400 ml of 0.16 M $Fe(NO_3)_3$ solution were first slowly mixed with 60 ml of 3 M NaOH. After 15 min, 217, 220 and 220 ml of 3 M NaOH were mixed into SFO-1-1, SFO-1-2 and SFO-1-4, respectively. The bottles were then closed, thoroughly shaken and stored at ~22 °C for 3 h (Lewis and Schwertmann, 1979). During this 3 h interval, 12 ml of 0.5 M $Al(NO_3)_3$ were slowly added to, and mixed with, 15 ml of 3 M NaOH (for use in SFO-1-2); and 60 ml of 0.5 M $Al(NO_3)_3$ were mixed with 88 ml of 3 M NaOH (for use in SFO-1-4). After 3 h, these two mixtures of $Al(NO_3)_3$ and NaOH were added to SFO-1-2 and SFO-1-4 (Table 1). All three polyethylene bottles were tightly closed, thoroughly shaken and stored in a laboratory oven at 48 °C for 5–19 days (Table 1).

Group 2: In each of three syntheses in this group (labeled as SFO-2-17, SFO-2-18 and SFO-2-19), 300 ml of 0.17 M $Fe(NO_3)_3$ solution were slowly mixed with 43 ml of 3.5 M NaOH. In a fourth polyethylene bottle (labeled SFO-2-20), 300 ml of 0.17 M $Fe(NO_3)_3$ solution were slowly mixed with 38 ml of 4 M NaOH. After 15 min, additional aliquots of 171, 150 and 150 ml of 3.5 M NaOH were slowly mixed into SFO-2-17, SFO-2-18 and SFO-2-19, respectively; whereas 140 ml of 4 M NaOH were slowly added into SFO-2-20. Deionized water was then added to SFO-2-17 to achieve a total solution volume of 600 ml. The four polyethylene bottles were closed, shaken and kept at ambient laboratory temperature of 22 °C for 3 h. During this 3 h, 11, 33 and 67 ml of 0.5 M $Al(NO_3)_3$ were added and mixed thoroughly with, respectively, 27 ml (for SFO-2-18) and 40 ml (for SFO-2-19) of 3.5 M NaOH; and 42 ml (for SFO-2-20) of 4 M NaOH. After 3 h, the solutions of $Al(NO_3)_3$ + NaOH prepared for SFO-2-18 and SFO-2-19 were added to the bottles containing those experiments. The remaining mixed solution of $Al(NO_3)_3$ + NaOH (made with 4 M NaOH) was added to SFO-2-20. Deionized water was then added to SFO-2-18, SFO-2-19 and SFO-2-20 to achieve solution volumes of 600 ml in each bottle. The polyethylene bottles were closed, thoroughly shaken and stored in the laboratory at 22 °C for 49 days. An aliquot of deionized water (~200 ml) used in the experiments was collected as "DIW-6" and stored in a Qorpak glass bottle with poly-seal screw cap.

2.1.2. Syntheses by method B: groups 3 and 4

Group 3: 8.29 g of $FeCl_2{\cdot}4H_2O$ reagent-grade powder were dissolved in 200 ml of deionized water in a Pyrex beaker (SFO-3-9). For SFO-3-12, 5.80 g of $FeCl_2{\cdot}4H_2O$ powder were mixed with 4.69 g of $Al(NO_3)_3{\cdot}9H_2O$ powder, the mixture was subsequently dissolved in 200 ml of deionized water in a Pyrex beaker. $FeCl_2$ was used, instead of $FeCl_3$, because the latter favors the formation of akaganeite from the aqueous solution in the experimental temperature range of 30–120 °C and low pH (e.g., Xu et al., 2002; Cornell and Schwertmann, 2003). In less than 10 min, each of these two solutions was transferred to a corresponding polyethylene bottle. The SFO-3-9 solution was added to a polyethylene bottle that contained 200 ml of 0.26 M $NaHCO_3$. The bottle to which SFO-3-12 solution was transferred contained 200 ml of 0.29 M $NaHCO_3$. Deionized water was added to each of the polyethylene bottles to achieve total solution volumes of 500 ml. Pure O_2 gas at one atmosphere pressure was bubbled for 2 min through the solutions in the polyethylene bottles using a glass tube immersed in the solutions. The polyethylene bottles were then closed, thoroughly shaken, and stored for 14 days in a laboratory oven maintained at 46 °C. An aliquot of deionized water used in the experiments was collected as "DIW-3" and stored in a Qorpak glass bottle with poly-seal screw cap.

Group 4: 7.46, 6.63 and 5.80 g of reagent-grade $FeCl_2{\cdot}4H_2O$ powder were mixed, respectively, with 1.56, 3.13 and 4.69 g of $Al(NO_3)_3{\cdot}9H_2O$ powder. These three mixtures were labeled, in succession, SFO-4-14, SFO-4-15 and SFO-4-16. The mixtures of powders were each dissolved in 200 ml of deionized water in Pyrex beakers. For experiment SFO-4-13, 8.29 g of $FeCl_2{\cdot}4H_2O$ were dissolved in 200 ml of deionized water with no addition of $Al(NO_3)_3{\cdot}9H_2O$. In less than 10 min, each of these four solutions was transferred to separate 1000 ml polyethylene bottles containing 200 ml of 0.26 M (for SFO-4-13), 0.27 M (for SFO-4-14), 0.28 M (for SFO-4-15) and 0.29 M (for SFO-4-16) $NaHCO_3$ solutions.

Table 1
The summary of conditions and results of synthesis experiments

Group #	Sample #[a]	Method[b]	T (°C)	Duration (days)	Initial					Final		Products		
					Fe^{3+} (M)	Na^{+} (M)	Al^{3+} (M)	$Al^{3+}/(Fe^{2+}+Al^{3+})$	pH	pH	Solution vol (ml)	Mineral[c]	Al mol % (XRD) (±3)	Al mol % (SEM) (±5–20%)[f]
1	SFO-1-1	A	48	5	0.09	1.23	0	0	~13–14	~13–14	677	G	0	0
	SFO-1-2	A	48	17	0.085	1.25	0.009	0.1	~13–14	~13–14	707	G	4	3
	SFO-1-4	A	48	19	0.072	1.35	0.036	0.33	~13–14	~13–14	828	G	7	9
2	SFO-2-17	A	22	49	0.08	1.25	0	0	14	14	600	G	0	0
	SFO-2-18	A	22	49	0.08	1.29	0.009	0.10	14	14	600	G	3	6
	SFO-2-19	A	22	49	0.08	1.36	0.028	0.26	14	14	600	G	8	11
	SFO-2-20	A	22	49	0.08	1.47	0.056	0.41	14	14	600	G	11	13
					Fe^{2+}									
3	SFO-3-9	B	46	14	0.084	0.103	0	0	6.5	4.5	500	G	0	0
	SFO-3-12	B	46	14	0.058	0.118	0.026	0.31	6	4	500	G + L(*m*)	10	12[d]
4	SFO-4-13	B	42	432	0.084	0.103	0	0	7.5	1.5	500	G + H(*m*)	0	0
	SFO-4-14	B	42	463	0.076	0.108	0.008	0.10	7.5	1.5	500	G + H(*m*)	4	6
	SFO-4-15	B	42	463	0.066	0.113	0.016	0.20	7.5	2.5	500	G + H(*m*) + L(*m*)	7	11
	SFO-4-16	B	42	463	0.058	0.118	0.026	0.31	7.5	2.5	500	G + H(*m*)	2, 15[e]	0, 15[e]

[a] First number behind "SFO" is group number, the 2nd is laboratory experiment number.
[b] A, solutes in initial solutions are: $Fe(NO)_3$, $Al(NO_3)_3$, NaOH; B, solutes in initial solutions are: $FeCl_2$, $Al(NO_3)_3$, $NaHCO_3$, O_2, see text.
[c] G, goethite; H, hematite; L, lepidocrocite; "*m*" denotes minor phase in the sample.
[d] After 5 M NaOH treatment at 22 ± 1 °C for 1 h. Total Al abundance in SFO-3-12 before treatment was ~28 mol %.
[e] Two estimated Al mol % values from XRD are based on the split peak of (1 1 1) of sample SFO-4-16, as shown in Fig. 3; the two data from SEM are from different locations in the sample that was used to acquire the SEM–EDAX image, see text.
[f] Percentage errors for the SEM data are *relative* errors as percentages of the nominal Al concentration. Uncertainties vary depending on the absolute abundance of the component, see text.

Deionized water was added to the polyethylene bottles to achieve solution volumes of 500 ml. Pure O_2 gas at one atmosphere pressure was bubbled for 2 min through each of the solutions in the polyethylene bottles using a glass tube immersed in the solutions. The polyethylene bottles were then closed, thoroughly shaken, and stored in an oven maintained at 42 °C for more than 400 days (Table 1). An aliquot of deionized water used in the experiments was collected as "DIW-4" and stored in a Qorpak glass bottle with poly-seal screw cap.

For all groups, the synthesis experiments were terminated by decanting the reaction water after centrifugal settling of the precipitate in closed Teflon tubes. The precipitate was then washed with de-ionized water until the pH of the rinse water remained unchanged at ~5.5 after rinsing. The washed precipitate was dried under vacuum at nominal room temperature (~22 ± 1 °C), comminuted and stored in Pyrex beakers covered with Pyrex watch glasses under ambient laboratory conditions for analysis.

2.2. Evaluation of the mineral composition of synthesis products

A Rigaku Ultima III X-ray diffraction (XRD) instrument was used to determine the mineral composition and the Al substitution of the synthesized samples. All patterns were obtained using CuKα radiation (40 kV, 44 mA) with Bragg–Brentano para-focusing beams. The height-limiting slit was set to 10 mm; both divergence slit and scattering slit were set to 2/3° and receiving-side slit was set to 0.45 mm. Samples were loaded into an aluminum holder using a back loading method to reduce preferred orientation. For mineral identification, samples were scanned at 1° 2θ/min in 0.05° steps over a range of 2θ from 2° to 70°. For determination of degrees of Al substitution for Fe in goethite, a scan rate of 0.1° 2θ/min with steps of 0.02° was used from 20° to 23° 2θ, and from 32° to 38.4° 2θ, to obtain, respectively, the "*d*" spacings of the (1 1 0) and (1 1 1) peaks (Schulze, 1984). The raw XRD patterns from the slow scans were analyzed with MDI Jade 7 software (part of Rigaku's analytical package) to standardize the procedure for locating the (1 1 0) and (1 1 1) peaks.

2.3. Determination of Al substitution in goethites

Schulze (1984) experimentally improved the method of determining the mol % of Al substituted for Fe in goethite using its XRD pattern. Because of the difference in size of the atoms (the Al^{3+} ion is 17% smaller than the Fe^{3+} ion), the unit cell dimensions of goethite crystals will systematically change with the degree of Al substitution, thus producing observed shifts of peaks (1 1 0) and (1 1 1) on an XRD pattern. The equation for the calculation of degree of Al substitution is (Schulze, 1984):

$$\text{Al mol\%} = 1730 - 572.0c \tag{3}$$

where,

$$c = \left[\left(\frac{1}{d(1\,1\,1)}\right)^2 - \left(\frac{1}{d(1\,1\,0)}\right)^2\right]^{-1/2} \tag{4}$$

"*d*" is the Bragg's Law *d*-spacing (in Å). The uncertainty in Al mol % calculated from Eq. (3) is about ±3 mol % (Schulze, 1984).

In this study, we also present chemical analyses of the samples by an SEM–EDAX energy-dispersive X-ray method. Analyses were performed using a Leo 1450VPSE with an EDAX Genesis 4000 XMS SYSTEM 60 energy-dispersive spectrometer at SMU. Powdered samples were attached to one side of a double sticking carbon tape whose other side is attached to an aluminum table. Firm pressing is necessary during the sample attachment to make sure the surface of the goethite powder is as smooth as possible. The table was then put into the SEM chamber, and pumped to a vacuum with internal pressure of less than 0.01 Pa. Multiple locations for EDAX analysis were selected from a 40× back-scatter image of each sample and an average value of Al mol % was then calculated in order to minimize the effects of possible sample heterogeneity and/or surface irregularities.

Limited internal calibration indicates that if the concentration of the element is >~ 1 mol %, the SEM–EDAX method for such powdered samples has a relative error of 5–20% when compared to wet chemical analyses. If the concentration of an element is less than 1 mol %, the relative error can be as high as 74%. Although less accurate than wet chemical methods, concentrations of Al determined by the energy dispersive method can be obtained rapidly and compared with Al concentrations determined for goethite by the method of Schulze (1984). If all of the Al in a sample were present as a substituent for Fe in the goethite structure, the percentage of Al in a sample as measured by the SEM–EDAX method should be the same (within analytical error) as the result from XRD patterns. On the other hand, if there were other Al phases in the sample, the SEM–EDAX result should yield higher Al abundances.

2.4. Measurements of D/H ratios

2.4.1. Measurement of D/H ratios of reaction water

Small aliquots (2–6 mg) of previously preserved deionized water were sealed into 0.4 mm I.D., 75 mm long glass capillary tubes. The water in a capillary tube was introduced into the vacuum extraction line using an evacuated, two part, "inverted T-shaped", reusable glass capillary "breaker". The water was frozen into a liquid nitrogen-cooled trap. The frozen water was purified by warming to dry ice-methanol temperature to remove CO_2. The H_2O was then passed through depleted uranium maintained at ~760 °C, which quantitatively converts the H_2O to H_2 gas. A Toepler pump was used to collect and measure the yield of the hydrogen gases (precision is ~± 1μmol). The stable hydrogen isotopic composition (δD) of collected hydrogen gas was measured on a Finnigan MAT 252 mass spectrometer in the stable isotope lab at SMU. The overall analytical precision of the method was ±2‰. δD is defined by:

$$\delta D = \left[\frac{(D/H)_{sample}}{(D/H)_{VSMOW}} - 1\right] \times 1000‰ \tag{5}$$

where, VSMOW = Vienna Standard Mean Ocean Water (Gonfiantini, 1978).

2.4.2. Measurement of D/H ratios of goethite structural hydrogen

Yapp and Poths (1995) suggested that there can be two categories of hydrogen remaining in a goethite sample that has been "outgassed" (in this study, "outgas" refers to the procedure of heating a sample to, and staying at, 100 °C for ~60 min in vacuum with continuous removal of recovered H_2O by freezing it in a liquid nitrogen-cooled trap). The two categories are: (1) structural hydrogen, which is isotopically non-exchangeable with ambient water vapor at room temperature on laboratory time scales; and (2) non-structural hydrogen (as "nonstoichiometric" water) which cannot be easily removed by outgassing without heating the sample to temperatures at which the goethite itself might break down. This latter type of hydrogen is termed "HTN" hydrogen, where "HTN" stands for "High Temperature Nonstoichiometric". The HTN hydrogen rapidly exchanges isotopes with ambient water at room temperature (Yapp and Poths, 1995). Boily et al. (2006), using FTIR spectroscopy, have identified nonstoichiometric hydrogen as deriving largely from excess water associated with the goethite. Goethite samples have different proportions of HTN hydrogen, and the HTN hydrogen complicates the determination of δD values of goethite structural hydrogen (δD_s). However, these difficulties can be overcome using the exchange procedure of Yapp and Poths (1995). The procedure is as follows. The goethite sample is outgassed successively at room T (60–120 min) and 100 °C (60–120 min) in vacuum in the dehydration chamber to remove adsorbed water and break down any amorphous synthetic ferrihydrite (Hsieh and Yapp, 1999). Then, "exchange water" of known initial amount and δD value is introduced into the system from a sealed capillary tube. This exchange water and the goethite sample remain together in the closed dehydration chamber at ~22 ± 1 °C for 18–18.5 h. Yapp and Poths (1995) found that exchange times of this order were sufficient to achieve apparent hydrogen isotope equilibrium between the HTN hydrogen and the ambient water introduced to the chamber. After exchange, the chamber and sample are outgassed again at room T and 100 °C in vacuum with the continuous collection of the evolved H_2O. This H_2O is cryogenically purified, converted to H_2 gas and measured for its yield and δD value. Finally, the goethite sample is dehydrated at 850 °C in closed system with 0.16 bar of O_2 with subsequent collection of H_2O for ~15 min. This 850 °C water is also cryogenically purified, converted to H_2 gas and measured for its yield and δD value as detailed in the preceding section.

The apparent hydrogen isotopic fractionation factor between HTN water and exchange water is termed "α_{e-v}". The hydrogen isotopic composition of the ambient water vapor plus adsorbed water (cumulative water recovered from the room T and 100 °C steps after exchange) is termed δD_v, which is mathematically related to the hydrogen isotopic composition of HTN hydrogen through α_{e-v}. Since the hydrogen isotopic composition of water extracted from goethite at 850 °C (δD_t) includes the contributions of both structural "nonexchangeable" hydrogen and exchangeable "HTN" hydrogen, δD_t will vary with variations in δD_v. Yapp and Poths (1995) predicted a linear relationship between δD_t and δD_v, as indicated in the equation below:

$$\delta D_t = m(1000 + \delta D_v) + b \tag{6}$$

where, $m = \alpha_{e-v}X_e$; $b = [\delta D_s - (1000 + \delta D_s)X_e]$; and X_e is the mole fraction of HTN hydrogen in the total hydrogen of the outgassed goethite. δD_s is the hydrogen isotopic composition of structural hydrogen. δD_t and δD_v are measured directly from exchange experiments. The respective values of α_{e-v}, X_e and δD_s should be constant among exchange experiments for a given sample. Thus, for a particular goethite sample, a series of exchange experiments using exchange waters with a different δD value for each aliquot of goethite should result in a linear relationship between δD_t and $(1000 + \delta D_v)$ with a slope of m and an intercept of b. Because the value of α_{e-v} is close to 1, the nominal value of "m" is approximately equal to, and no more than 5–6% lower than, the proportion of HTN hydrogen (X_e) in the goethite (Eq. (6)).

The value of δD_s can be calculated from the results of the exchange experiments using the equation below (Yapp and Poths, 1995):

$$\delta D_s = \frac{1}{\left(1 - \frac{m}{\alpha_{e-v}}\right)}\left(b + 1000\frac{m}{\alpha_{e-v}}\right) \tag{7}$$

A value of α_{e-v} of 0.996 (±0.04) was determined for some goethite samples by Yapp and Poths (1995), where the calculated δD of only the vapor component of the exchange water was used to determine α_{e-v}. However, Yapp (1997) found that this value of α_{e-v} may not be applicable for all goethites. These uncertainties in the value of α_{e-v} indicate the necessity of the re-evaluation of the value of α_{e-v} in the current study, because for large measured values of "m", the calculated values of δD_s are very sensitive to the value of α_{e-v} (Eq. (7)). Once the δD_s is determined, the hydrogen isotopic fractionation factor between the non-exchangeable structural hydrogen in goethite and the hydrogen in ambient liquid water of the synthesis experiments ($^D\alpha_{G-W}$) can be obtained from:

$$^D\alpha_{G-W} = \frac{1000 + \delta D_s}{1000 + \delta D_W} \tag{8}$$

δD_W is the hydrogen isotopic composition of the reaction water used in corresponding synthesis experiments.

2.5. Chemical treatment

Subsequent to synthesis, one goethite sample (SFO-3-12) was treated with 5 M NaOH at room temperature (22 ± 1 °C) for 1 h to dissolve any Al oxide and/or oxyhydroxide phases in the sample. The probable existence of such phases was inferred, because (before NaOH treatment) the Al abundance determined using SEM–EDAX was significantly higher than that determined by the XRD method (Table 1). The 5 M NaOH treatment at 100 °C has been tested on natural goethite samples, and shown not to affect the $\delta^{18}O$ of the structural oxygen in goethite (Yapp, 1991).

However, the effect of this 5 M NaOH treatment at 22 °C on the hydrogen isotopic composition of structural hydrogen in synthetic goethite has not been tested.

3. RESULTS AND DISCUSSION

3.1. Mineral products

The minerals identified in these samples are listed in Table 1. An illustrative XRD pattern (SFO-4-15) is shown in Fig. 1. For 8 of 13 samples of Table 1, goethite is the only detectable mineral. For the remaining 5 samples (groups 3 and 4), hematite is found in 4 samples and lepidocrocite is found in 2 samples in minor amounts (Table 1). Hematite does not have hydrogen in its structure, and the influence of lepidocrocite on the D/H exchange experiments is expected to be small due to its small abundance.

The crystal sizes of all of the goethites synthesized for this study are small (<600 nm). However, SEM photos indicate that the samples in groups 3 and 4 (Fig. 2d and e), which were synthesized at 42–46 °C by the Fe^{2+} oxidation method (method B) in mid to low pH solutions (final pH is 1.5–4.5), tend to have crystals which are generally smaller, and more varied in size and shape, than those of groups 1 and 2. The generally longer and more uniformly shaped crystals in samples of groups 1 and 2 (Fig. 2a–c) were synthesized by the Fe^{3+} hydrolysis method (method A) in high pH solutions (final pH is 13–14) at 22–48 °C.

The results of Schwertmann and Murad (1983) indicate that the half conversion time (HCT) from ferrihydrite to goethite by dissolution and crystallization varies significantly with pH. At an experimental temperature of 24 °C and a pH of 12, HCT is <4 days, while at a pH of 2.5 and 24 °C, the HCT is ~354 days. These results suggest that there will be minimal amounts of ferrihydrite associated with goethite from the syntheses of the current study that were performed at high pH (13–14) and temperatures of 48 °C (5–19 days) in group 1, and at high pH (14) and temperatures of 22 °C (49 days) in group 2. If the "rule of thumb" that reaction rates approximately double for every increase in temperature of 10 °C is applicable (Barrow, 1966), the HCT for group 1 should be <1 day. Thus, a synthesis time of only 5 days in SFO-1-1 of group 1 should represent 5 or more HCT's. If so, ferrihydrite in this sample, as an example, should constitute <3% of the final sample. In contrast, the mid- to low-pH syntheses (groups 3 and 4) may contain higher proportions of ferrihydrite. However, the initial outgassing of each sample at 100 °C in vacuum prior to an exchange experiment should convert most, or all, of any admixed synthetic ferrihydrite to hematite (e.g., Hsieh and Yapp, 1999).

3.2. Al substitution

The inferred Al mol % ranges from 0 to 15% and, except for the initial Al/(Fe + Al) ratio in the solutions, does not seem to be related to the conditions under which the goethite formed (Table 1). Although generally positive, the correlation between initial Al/(Fe + Al) in the solutions and Al mol % in the products is not linear. For all samples except one, the corresponding mol % values for Al inferred from SEM–EDAX and XRD agree with each other within the analytical uncertainties (Table 1). This supports an assumption that the degree of Al substitution inferred from XRD analysis is reliable, and that (with one exception) there are no other Al phases in these samples. The exception is sample SFO-3-12.

Prior to treatment with 5 M NaOH, SEM–EDAX results for SFO-3-12 showed elevated levels of Al (28% compared to the 10% inferred from the XRD pattern). This indicated the existence of one, or more discrete Al phases in SFO-3-12. The treatment of SFO-3-12 with 5 M NaOH

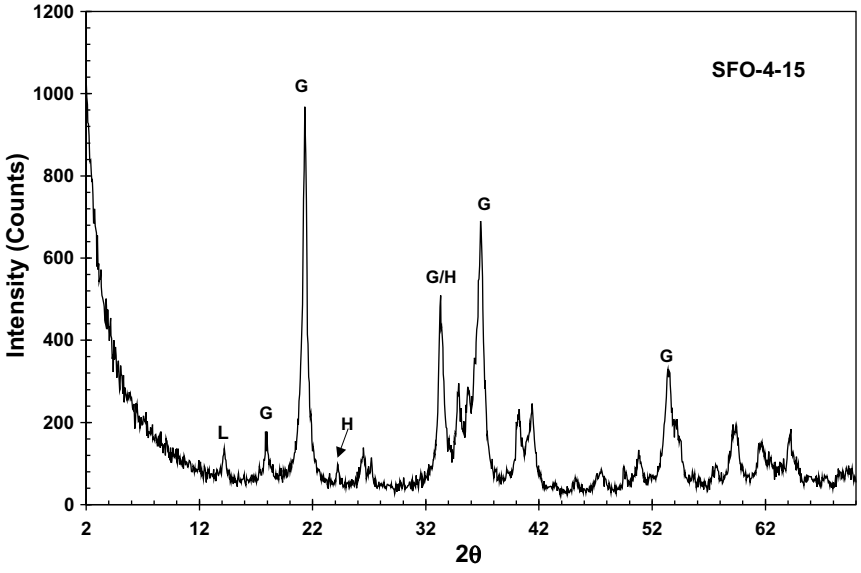

Fig. 1. The XRD pattern for synthesized goethite sample. This sample (SFO-4-15) is the only synthetic sample in this study with three minerals detected under XRD. G, goethite; H, hematite; L, lepidocrocite, mineral composition of each sample is listed in Table 1.

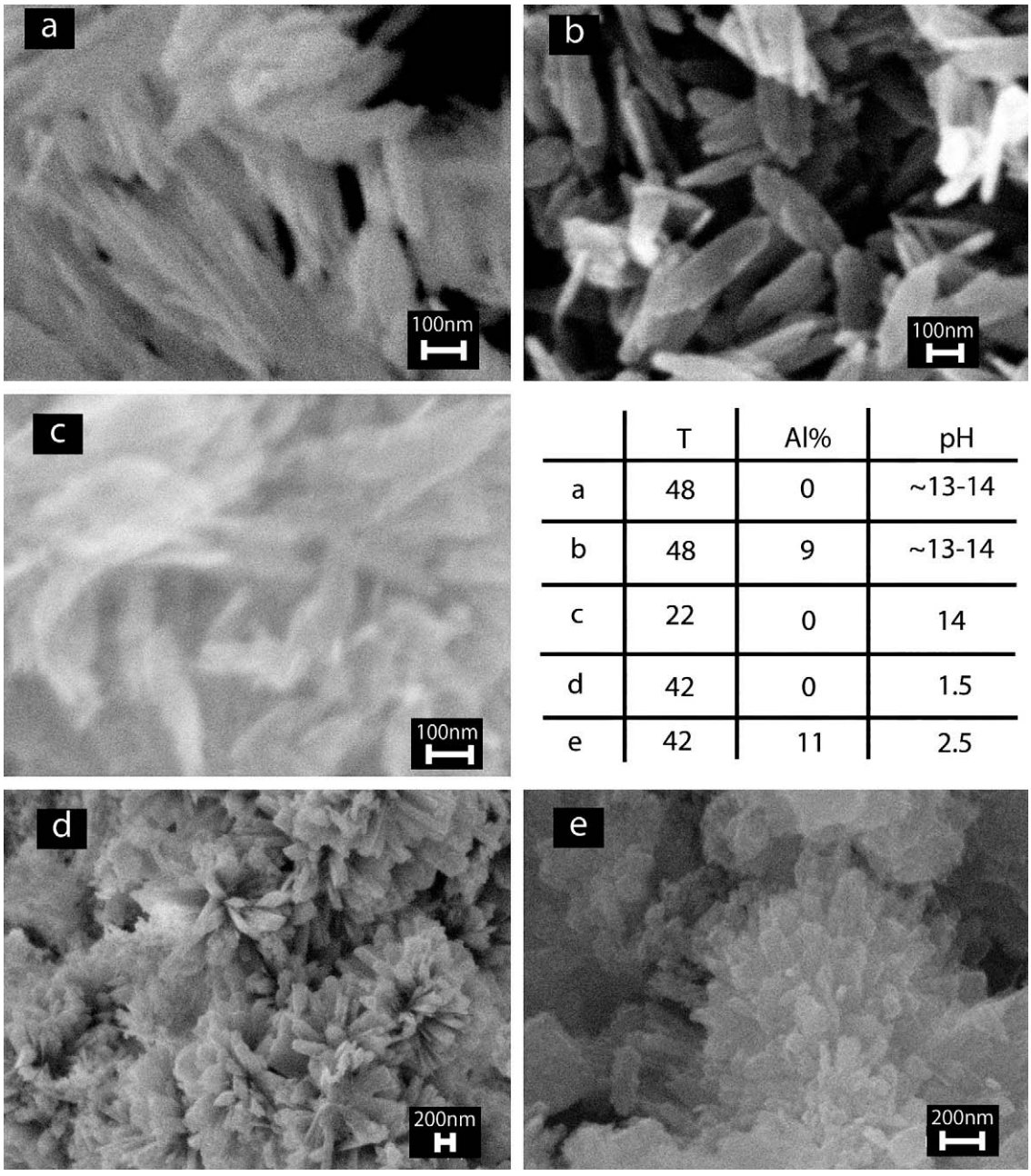

	T	Al%	pH
a	48	0	~13-14
b	48	9	~13-14
c	22	0	14
d	42	0	1.5
e	42	11	2.5

Fig. 2. SEM photos of synthesized sample discussed in this study. (a) SFO-1-1; (b) SFO-1-4; (c) SFO-2-17; (d) SFO-4-13; (e) SFO-4-15. Samples in (a–c) were synthesized by the method of hydrolysis of Fe^{3+} in solutions with pH values of 13–14 at temperatures of 22–48 °C. Samples in (d) and (e)were synthesized in solutions of low pH values of 1.5–2.5 by the method of oxidation of Fe^{2+} at a temperature of 42 °C. The scale bars in all photos are 100 or 200 nm as illustrated. "Al %" is the Al substitution for Fe in synthesized goethite as measured by its XRD pattern.

at room temperature for 1 h effectively removed the excess Al phases as indicated by an SEM–EDAX value of 12 mol % Al in SFO-3-12 after the treatment. This latter value is in accord (within analytical uncertainty) with the value for the concentration of Al substituted for Fe in goethite as determined by XRD analysis (Table 1).

A different complication was exhibited by sample SFO-4-16. It has a split (1 1 1) peak in its XRD pattern, which appears to correspond to two different groups of goethites in the sample with different degrees of Al substitution (2 and 15 mol %; see Fig. 3 and Table 1). This heterogeneity of Al mol % of the sample was also observed in SEM–EDAX analyses. Such analyses of different locations in SFO-4-16 showed two populations of Al mol % at ~0% and ~15%. These values agree within analytical uncertainty with those determined by XRD. Because of this complication of two degrees of Al substitution, SFO-4-16 was not included in the exchange experiments.

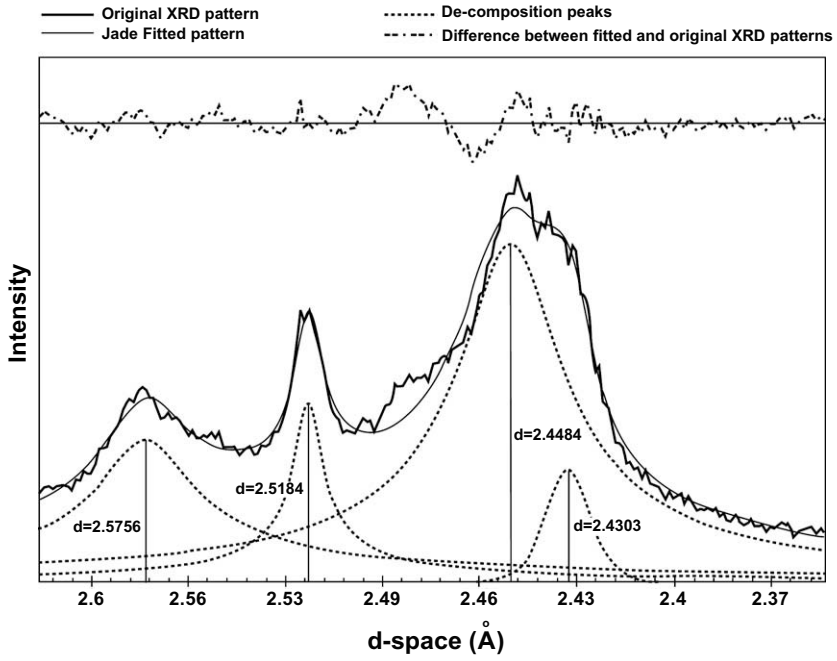

Fig. 3. The split (1 1 1) peak of sample SFO-4-16, and the peak positions were located through the peak decomposition/peak fit function in MDI Jade 7 software. The two peaks correspond to two different Al mol %, which are 2% and 15%, respectively.

3.3. Hydrogen isotopic fractionation between ambient water and synthesized goethites with different degrees of Al substitution

3.3.1. Results from exchange experiments

The hydrogen isotope data from the exchange experiments (Table 2) are plotted in Figs. 4a, b and 5a, b. The results of the exchange experiments define specific linear relationships between δD_t and $(1000 + \delta D_v)$ for each sample in the four groups. Regression parameters for all samples are listed in Table 3. According to Eq. (7), the slopes and intercepts of these regressions can be used to determine the δD_s values for various goethites if the value of α_{e-v} is known. As noted previously, with this δD_s value and knowledge of the δD_W of the reaction water (Table 3), ${}^{D}\alpha_{G-W}$ can be calculated using Eq. (8).

3.3.2. The existence of effects of Al substitution on the ${}^{D}\alpha_{G-W}$

To evaluate the effect of Al substitution on the fractionation factor between water and goethite, $1000\ln {}^{D}\alpha_{G-W}$ (calculated using Eqs. (7) and (8)) was plotted against X_{Al} (Al substitution expressed as the mole fraction, Al/(Al + Fe), in the sample) for groups 2, 3 and 4. The δD_W of reaction water for group 1 is unknown and the estimation of the effects of Al substitution on ${}^{D}\alpha_{G-W}$ for this group will be discussed in the next section. The value of α_{e-v} used in Eq. (7) was temporarily assumed to be 0.996 (Yapp and Poths, 1995) and was used to determine the values of δD_s (Table 4) that led to Eqs. (9)–(11).

Linear regressions of the data for groups 2, 3 and 4 (for an α_{e-v} value of 0.996) yield:

$$\text{Group 2}: 1000\ln {}^{D}\alpha_{G-W} = 141(\pm 18)X_{Al} - 126(\pm 1),\quad r^2 = 0.97 \tag{9}$$

$$\text{Group 3}: 1000\ln {}^{D}\alpha_{G-W} = -160X_{Al} - 121,\quad (2\text{ point regression}) \tag{10}$$

$$\text{Group 4}: 1000\ln {}^{D}\alpha_{G-W} = -130(\pm 14)X_{Al} - 123(\pm 1),\quad r^2 = 0.99 \tag{11}$$

The positive slope of group 2 is consistent with the prediction of a positive slope using the thermodynamic model (Eq. (2)). However, the slopes for groups 3 and 4 are negative. This lack of consistency in the slopes of Eqs. (9)–(11) suggests that the determination of the δD_s values of these samples needs to be further evaluated.

The value of 0.996 for α_{e-v} has a significant uncertainty of ±0.04 in the experiments of Yapp and Poths (1995). Because the values determined for δD_s (and thus, also the calculated ${}^{D}\alpha_{G-W}$ value) are sensitive to the choice of α_{e-v} for large values of "*m*", and because the values of "*m*" differ significantly among the samples of groups 3 and 4 (Fig. 5), it might be expected that the deduced relationships between $1000\ln {}^{D}\alpha_{G-W}$ and X_{Al} would also depend on the value of α_{e-v}.

The four sample sets in group 2 all have slopes ("*m*", Eq. (6)) for the exchange experiments that are almost parallel with each other (Fig. 4b). This indicates that the various sample sets in this group have comparable proportions of HTN hydrogen. For the contrasting slopes among the sample sets of groups 3 and 4, "*m*" generally increases with increasing degree of Al substitution (Table 3) indicating higher proportions of HTN hydrogen in the samples with higher Al substitution. These differences in the proportions of HTN water among goethites within groups 3 and 4 will

Table 2
Data from hydrogen isotope exchange experiments at 22 °C

Group #	Sample #	MHD[a] #	Sample mass[b] (mg)	Exchange conditions				Goethite 850 °C H_2O			Final exchange H_2O	
				Initial exchange H_2O			22 °C exchange time (min)					
				μmol (tot.)	δD (‰)	% (v)[c]		μmol	δD (‰)	wt.%	μmol[d]	δD (‰)
1	SFO-1-1	2263	38.8	194	−252	76	1110	240	−149	11.1	159	−198
	SFO-1-1	2266	37.5	111	−178	62	1110	231	−133	11.1	95	−134
	SFO-1-1	2278	40.8	167	114	88	1108	256	−84	11.3	138	40
	SFO-1-2	2281	38.3	178	114	80	1110	243	−77	11.4	140	40
	SFO-1-2	2283	39.8	150	−252	75	1110	253	−138	11.5	124	−169
	SFO-1-2	2287	42.7	156	−252	70	1110	270	−144	11.4	128	−182
	SFO-1-2	2288	38.6	178	−252	82	1110	241	−145	11.2	148	−194
	SFO-1-2	2284	42.1	128	−178	71	1110	269	−133	11.5	109	−142
	SFO-1-4	2269	39.3	156	−252	83	1110	252	−146	11.6	124	−196
	SFO-1-4	2272	43.4	161	−178	83	1110	278	−136	11.5	133	−161
	SFO-1-4	2276	39.0	172	114	85	1110	251	−78	11.6	139	35
2	SFO-2-17	2441	54.4	194	−252	42	1080	327	−147	11.0	177	−174
	SFO-2-17	2426	54.8	211	114	51	1080	324	−85	10.7	202	58
	SFO-2-17	2436	56.4	222	−178	51	1080	334	−139	10.6	208	−135
	SFO-2-17	2438	55.6	233	22	54	1080	333	−107	10.7	216	−16
	SFO-2-18	2446	57.1	211	−252	47	1080	350	−149	11.0	188	−185
	SFO-2-18	2430	53.2	183	114	49	1080	324	−82	10.9	173	40
	SFO-2-18	2447	49.1	239	−178	60	1080	297	−137	10.8	211	−146
	SFO-2-18	2448	52.9	222	22	54	1080	322	−100	11.0	198	−13
	SFO-2-19	2443	56.2	211	−252	53	1080	351	−144	11.4	189	−184
	SFO-2-19	2433	54.6	200	114	58	1080	346	−77	11.6	181	42
	SFO-2-19	2437	55.1	228	−178	64	1080	347	−135	11.5	206	−146
	SFO-2-19	2450	53.4	206	22	57	1080	338	−97	11.5	184	−19
	SFO-2-20	2444	49.3	217	−252	60	1080	311	−145	11.5	191	−191
	SFO-2-20	2435	54.7	178	114	53	1080	346	−79	11.4	173	31
	SFO-2-20	2449	50.7	189	−178	55	1080	323	−131	11.5	167	−137
	SFO-2-20	2451	52.3	189	22	50	1080	333	−95	11.4	170	−14
3	SFO-3-9	2315	38.9	150	−178	75	1107	219	−130	10.2	127	−141
	SFO-3-9	2318	39.5	150	114	43	1107	217	−89	10.0	129	47
	SFO-3-9	2320	41.4	156	−252	77	1107	226	−140	9.9	134	−182
	SFO-3-12	2453	44.9	200	−252	50	1080	269	−155	11.0	178	−170
	SFO-3-12	2455	39.1	206	22	59	1080	230	−82	10.6	181	−9
	SFO-3-12	2454	38.1	217	114	60	1080	223	−65	10.7	189	34

4	SFO-4-13	2397	52.8	183	−252	78	1110	277	−143	9.5	151	−203
	SFO-4-13	2398	50.0	189	114	80	1110	266	−93	9.6	151	41
	SFO-4-13	2399	52.2	211	−178	80	1110	274	−133	9.5	171	−154
	SFO-4-14	2402	44.8	200	−252	65	1110	246	−153	9.9	178	−201
	SFO-4-14	2403	51.3	200	114	58	1110	283	−90	10.0	177	28
	SFO-4-14	2404	42.2	194	22	64	1110	233	−97	10.0	171	−13
	SFO-4-15	2405	49.9	189	114	37	1110	269	−75	9.8	175	30
	SFO-4-15	2406	40.7	200	22	50	1110	222	−89	9.9	183	−14
	SFO-4-15	2407	38.5	217	−252	56	1110	212	−155	10.0	192	−184

[a] MHD # is internal laboratory numbers, for reference only.
[b] Mass of sample after "outgassing" at room T and 100 °C, see text.
[c] The proportion of exchange water that is in vapor phase.
[d] The final exchange water is from dehydration chamber and represents water vapor plus adsorbed water. 79-96% of the all water introduced into the system. See text.

Fig. 4. δD_t vs. $(1000 + \delta D_v)$ for groups 1 and 2 of synthesized goethite samples. Data are listed in Table 2. Solid lines represent the regressions performed for the sample sets; regression parameters are listed in Table 3.

Fig. 5. δD_t vs. $(1000 + \delta D_v)$ for groups 3 and 4 of synthesized goethite samples. Data are listed in Table 2. Solid lines represent the regressions performed for the sample sets; regression parameters are listed in Table 3.

Table 3
Linear regression parameters for: $\delta D_t = m(1000 + \delta D_v) + b$

Group #	Sample #	Al mol % (XRD)	m[a,b]	b[a]	r[b]	Measured δD of reaction water	
						Sample #	δD_W (±2) ‰
1	SFO-1-1	0	0.2743 (±0.0067)	−370 (±6)	0.999	—	—
	SFO-1-2	4	0.2953 (±0.0085)	−385 (±7)	0.998	—	—
	SFO-1-4	7	0.2954 (±0.0009)	−384 (±1)	~1	—	—
2	SFO-2-17	0	0.2684 (±0.0086)	−370 (±8)	0.998	DIW-6	−22
	SFO-2-18	3	0.2932 (±0.0070)	−388 (±6)	0.998	DIW-6	−22
	SFO-2-19	8	0.2971 (±0.0078)	−388 (±7)	0.998	DIW-6	−22
	SFO-2-20	11	0.2959 (±0.0088)	−385 (±8)	0.998	DIW-6	−22
3	SFO-3-9	0	0.2209 (±0.0042)	−320 (±4)	~1	DIW-3	−14
	SFO-3-12	10	0.4457 (±0.0088)	−525 (±8)	~1	DIW-3	−14
4	SFO-4-13	0	0.2053 (±0.0001)	−307 (±0.1)	~1	DIW-4	−13
	SFO-4-14	4	0.2819 (±0.0189)	−378 (±18)	0.996	DIW-4	−13
	SFO-4-15	7	0.3780 (±0.0132)	−463 (±13)	0.999	DIW-4	−13

[a] Uncertainties in the slopes and intercepts arise from the scatter in the nominal values of the measured data.
[b] The excess significant figures in "m" are reported because they were used to avoid rounding errors in the calculation of δD_s values. The calculated values of δD_s, however, are rounded to the nearest whole number. An r^2 of "~1" indicates that rounding to 3 digits to the right of the decimal point will result in a value of 1.

Table 4
The calculation for δD_s and $^D\alpha_{G-W}$ using different values of α_{e-v}

Group #	Sample #	Al%			$\alpha_{e-v} = 0.996$		$\alpha_{e-v} = 0.942$		
		(XRD)	(SEM)	δD_W‰[a]	δD_s[b]	$1000 \ln {}^D\alpha_{G-W}$	δD_s[b]	$^D\alpha_{G-W}$[c]	$1000 \ln {}^D\alpha_{G-W}$
1	SFO-1-1	0	0	−12	—	—	−111	0.900	−105
	SFO-1-2	4	3	−12	—	—	−104	0.907	−98
	SFO-1-4	7	9	−12	—	—	−103	0.908	−97
2	SFO-2-17	0	0	−22	−138	−127	−119	0.901	−104
	SFO-2-18	3	6	−22	−133	−120	−111	0.909	−95
	SFO-2-19	8	11	−22	−128	−114	−106	0.914	−90
	SFO-2-20	11	13	−22	−125	−111	−103	0.917	−87
3	SFO-3-9	0	0	−14	−126	−121	−112	0.901	−104
	SFO-3-12	10	12	−14	−140	−137	−98	0.915	−89
4	SFO-4-13	0	0	−13	−127	−123	−114	0.898	−108
	SFO-4-14	4	6	−13	−132	−129	−112	0.900	−105
	SFO-4-15	7	11	−13	−135	−132	−103	0.909	−95

[a] $\delta D_W = -12‰$ for samples of group 1 is an estimated value; see text.
[b] δD_s values are calculated using Eq. (7); see text.
[c] $^D\alpha_{G-W}$ values are calculated using Eq. (8), the results for samples in group 1 are based on the assumption of $\delta D_W = -12‰$. See text.

amplify the sensitivity of $^D\alpha_{G-W}$, as well as relationships between $1000 \ln {}^D\alpha_{G-W}$ and X_{Al}, to the choice of α_{e-v} (Eq. (7)). In the subsequent discussion, the following expression is assumed to be relevant:

$$1000 \ln {}^D\alpha_{G-W} = CX_{Al} + D \quad (12)$$

where "C" and "D" are, respectively, the slope and intercept.

To evaluate the effects of variations of α_{e-v} on the magnitude of the slope ("C"), we specified different values of α_{e-v} and calculated the corresponding regression slopes for each of three groups for which δD_W was measured (i.e., Groups 2, 3 and 4). For a particular group, eleven α_{e-v} values in increments of 0.01 over the range from 0.900 to 1.000 were applied to all samples in the group. The specified range of α_{e-v} values was suggested by values of $^D\alpha_{G-W}$ and α_{e-v} reported in Yapp and Pedley (1985) and Yapp (1987, 1997). For each value of α_{e-v}, the δD_s and $^D\alpha_{G-W}$ values for all samples in a group were calculated using Eqs. (7) and (8). A linear regression of $1000 \ln {}^D\alpha_{G-W}$ vs. X_{Al} for a group was then performed for each choice of α_{e-v} to determine the value of "C" that corresponded to the chosen α_{e-v} value. The values of "C" generated in this manner are plotted against α_{e-v} in Fig. 6 for each of the three groups. For group 2, "C" is relatively insensitive to the choice of α_{e-v}. In contrast, for groups 3 and 4, "C" is highly sensitive to

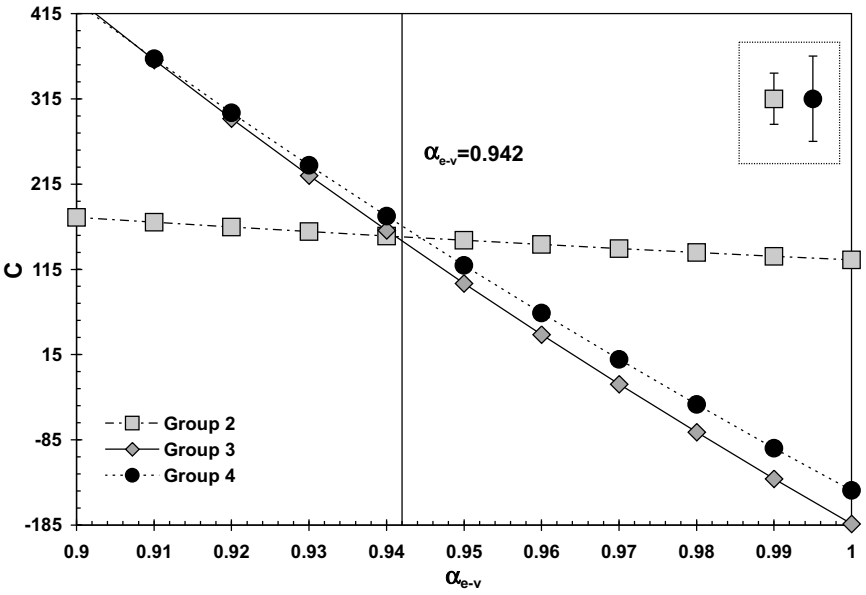

Fig. 6. The effects of different choices of value of $\alpha_{e\text{-}v}$ on the slope ("*C*") of $1000\ln {}^{D}\alpha_{G\text{-}W}$ vs. X_{Al} for groups 2, 3 and 4. The vertical dotted line depicts the value of α_{e-v} at which all three groups of goethites exhibit similar slopes on a plot of $1000\ln {}^{D}\alpha_{G-W}$ vs. X_{Al}. The uncertainties are illustrated in the upper right dotted box.

the choice of α_{e-v}, because of the large proportions of HTN water in these samples and the variation of these proportions with the degree of Al substitution.

The relative insensitivity of "*C*" to the choice of $\alpha_{e\text{-}v}$ for group 2 (Fig. 6) over a range of $\alpha_{e\text{-}v}$ from 0.900 to 1.000 implies that the positive correlation between $1000\ln {}^{D}\alpha_{G-W}$ and X_{Al} observed for group 2 is a consequence of the thermodynamic effects of substitution of Al for Fe in goethite and is *not* an artifact of the behavior of HTN water. Fig. 6 also suggests a basis for estimating a numerical value for α_{e-v} that characterizes all of the experimental groups of this study.

3.3.3. The determination of α_{e-v}

If Al substitution has a consistent effect on $1000\ln {}^{D}\alpha_{G-W}$ for all of these synthetic goethites, irrespective of the method and conditions of synthesis (i.e., similar "*C*" for all groups), Fig. 6 suggests that all of these goethites could exhibit about the same value of α_{e-v}. The value of α_{e-v} which satisfies this condition is determined by the approximate point of mutual intersection of the three curves of Fig. 6. This common value of α_{e-v} is about 0.942 (±0.02) and corresponds to a "*C*" value of ~140 for all three groups of Fig. 6.

Application of a nominal value for α_{e-v} of 0.942 to the goethites containing no Al (SFO-2-17, SFO-3-9 and SFO-4-13) yields calculated values of ${}^{D}\alpha_{G-W}$ of 0.901 (±0.006), 0.898 (±0.005) and 0.901 (±0.008), respectively, which are in agreement (within experimental error) with the published value of 0.905 (±0.004) (Yapp and Pedley, 1985; Yapp, 1987). This agreement seems to validate a value of 0.942 (at 22 °C) as a reasonable estimation of the value of α_{e-v} for this study. This ${}^{D}\alpha_{G-W}$ value of 0.900 (±0.006) was determined without any priori assumptions about the attainment of hydrogen isotopic equilibrium between structural hydrogen and synthesis water. Therefore, the average ${}^{D}\alpha_{G-W}$ value of 0.900 (±0.006) indicates that goethites synthesized in this study approached hydrogen isotopic equilibrium to about the same degree as goethites in the published experiments (i.e., 0.905 ± 0.004).

As mentioned above, the reaction water for group 1 was not preserved. However, with an α_{e-v} value of 0.942 and an ${}^{D}\alpha_{G-W}$ value of 0.900 (the average value of calculated ${}^{D}\alpha_{G-W}$ determined for SFO-2-17, SFO-3-9 and SFO-4-13), the δD_W for group 1 can be calculated. Eqs. (7) and (8) and the δD_s value from the results of the exchange experiments for SFO-1-1 (the Al-free goethite in group 1) were used to determine a δD_W value of −12 (±8)‰ for group 1. This value is in approximate agreement with the measured range of δD_W values of the other three groups (Table 4). It should be noted that the deionized water (δD_W) was taken at different times from the local building supply to initiate these various groups of goethite syntheses and the δD of that water varies depending on the variation of δD of the input water prior to deionization.

A value of 0.942 (±0.02) for α_{e-v} indicates a rather large apparent deuterium depletion in HTN hydrogen relative to ambient water. Among the various exchange experiments, the vapor constitutes from 37% to 88% (Table 2) of the total exchange water. These percentages were determined by measuring amounts of vapor in small volumes connected to the dehydration chamber during the exchange experiments. The known ratio of these small volumes to the volume of the chamber should be equal to the ratio of amounts of vapor in the small volumes to vapor in the chamber. Knowledge of total water added to the system allowed a determination (by a simple difference calculation) of the amount of such water presumably adsorbed on the goethite. This permitted the estimation of the percentage of exchange water actually present as vapor. If the exchange

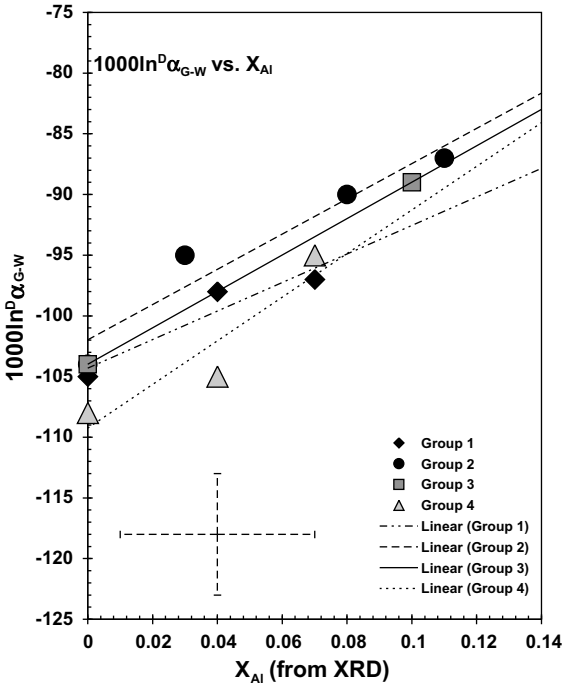

Fig. 7. $1000\ln {}^{D}\alpha_{G\text{–}W}$ vs. X_{Al} using an estimated $\alpha_{e\text{–}v}$ of 0.942 (see text). Uncertainties are indicated in the lower left. The X_{Al} data are from XRD. Regression equations are:

$$\text{Group 1}: 1000\ln {}^{D}\alpha_{G\text{–}W} = 118\ (\pm 40)X_{Al} - 104\ (\pm 2), \quad r^2 = 0.90$$
$$\text{Group 2}: 1000\ln {}^{D}\alpha_{G\text{–}W} = 145\ (\pm 30)X_{Al} - 102\ (\pm 2), \quad r^2 = 0.93$$
$$\text{Group 3}: 1000\ln {}^{D}\alpha_{G\text{–}W} = 150X_{Al} - 104, \quad \text{(2 point regression)}$$
$$\text{Group 4}: 1000\ln {}^{D}\alpha_{G\text{–}W} = 180\ (\pm 73)X_{Al} - 109\ (\pm 3), \quad r^2 = 0.86$$

water as a whole behaves as a mixture of two phases (vapor and adsorbed water) with D/H ratios which differ by some equilibrium fractionation (α_{eq}), it would imply that the $\alpha_{e\text{–}v}$ determined for these experiments is a composite value. The significance of this possibility will be discussed in the following section.

3.3.4. Summary of the effects of Al substitution on the ${}^{D}\alpha_{G\text{–}W}$

With the nominal value of 0.942 estimated for $\alpha_{e\text{–}v}$, ${}^{D}\alpha_{G\text{–}W}$ was calculated using Eqs. (7) and (8) for all samples. As mentioned, a δD_W value of $-12‰$ was used to calculate ${}^{D}\alpha_{G\text{–}W}$ for group 1 (Table 4). Plots of resulting values of $1000\ln {}^{D}\alpha_{G\text{–}W}$ against X_{Al} are shown in Fig. 7. Linear regressions for the various groups yielded the following equations:

$$\text{Group 1}: 1000\ln {}^{D}\alpha_{G\text{–}W} = 118(\pm 40)X_{Al} - 104(\pm 2), \quad r^2 = 0.90 \tag{13}$$
$$\text{Group 2}: 1000\ln {}^{D}\alpha_{G\text{–}W} = 145(\pm 30)X_{Al} - 102(\pm 2), \quad r^2 = 0.93 \tag{14}$$
$$\text{Group 3}: 1000\ln {}^{D}\alpha_{G\text{–}W} = 150X_{Al} - 104, \quad \text{(2 point regression)} \tag{15}$$
$$\text{Group 4}: 1000\ln {}^{D}\alpha_{G\text{–}W} = 180(\pm 73)X_{Al} - 109(\pm 3), \quad r^2 = 0.86 \tag{16}$$

The uncertainties indicated in Eqs. (13)–(16) reflect the scatter of the nominal values of the data points; they do not include the errors caused by individual uncertainties of X_{Al} and $1000\ln {}^{D}\alpha_{G\text{–}W}$.

The results for all four groups of experiments are plotted collectively in Fig. 8a (X_{Al} determined by XRD, Schulze, 1984). For comparison, the values of $1000\ln {}^{D}\alpha_{G\text{–}W}$ for all four groups are also plotted against values for X_{Al} obtained from the SEM–EDAX method in Fig. 8b. The respective regressions yield the following equations:

$$\text{XRD (Fig.8a)}: 1000\ln {}^{D}\alpha_{G\text{–}W} = 159(\pm 23)X_{Al} - 105(\pm 1), \quad r^2 = 0.83 \tag{17}$$
$$\text{SEM – EDAX (Fig.8b)}: 1000\ln {}^{D}\alpha_{G\text{–}W} = 122(\pm 19)X_{Al} - 105(\pm 1), \quad r^2 = 0.80 \tag{18}$$

Within the analytical uncertainties, the regression lines of Eqs. (17) and (18) are in good agreement. However, both slopes are somewhat larger than the slope predicted by the published model (Yapp, 1993; dashed line in Fig. 8a and b).

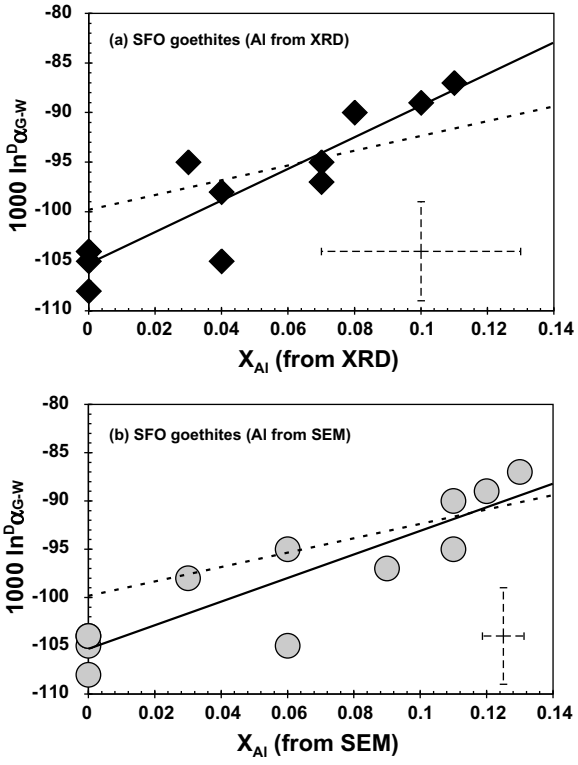

Fig. 8. Summary of $1000\ln {}^{D}\alpha_{G\text{–}W}$ vs. X_{Al} for all the samples from groups 1, 2, 3 and 4. Solid lines represent the regression lines for all samples discussed. Dashed lines are redrawn from the thermodynamic mixing model of Yapp, 1993. Uncertainties are indicated in the lower right of each plot. (a) Using the Al mole fraction measured with the XRD method (Schulze, 1984); (b) Using the Al mole fraction measured with the SEM–EDAX method (see text). The two regression lines with different methods of determination of Al mole fraction are:

$$\text{From XRD}: 1000\ln {}^{D}\alpha_{G\text{–}W} = 159\ (\pm 23)X_{Al} - 105\ (\pm 1), \quad r^2 = 0.83$$
$$\text{From SEM}: 1000\ln {}^{D}\alpha_{G\text{–}W} = 122\ (\pm 19)X_{Al} - 105\ (\pm 1), \quad r^2 = 0.80$$

This difference might arise from: (1) the necessity of using boehmite instead of diaspore for the AlOOH endmember in the model calculation; (2) error arising from the ideal solid solution approximation; (3) rather than being a constant, the value of α_{e-v} in these exchange experiments might itself be influenced by either degrees of Al substitution or distribution of exchange waters in two different phases.

A sensitivity calculation assuming that $1000\ln\alpha_{e-v}$ varies with X_{Al} to about the same degree as that predicated by the thermodynamic model for goethite (slope of 74, for Al as a mole fraction) yields resultant values of $^{D}\alpha_{G-W}$ which indicate that a plot of $1000\ln{}^{D}\alpha_{G-W}$ vs. X_{Al} would have a slope of ~117 with an r^2 of 0.73. Therefore, although such a dependence of α_{e-v} on X_{Al} would yield a change in the deduced magnitude of the dependence of $1000\ln{}^{D}\alpha_{G-W}$ on X_{Al} (e.g., a slope about 26% lower), the pattern of increasing $1000\ln{}^{D}\alpha_{G-W}$ with increasing X_{Al} would still be evident.

The consequences for interpretation of the data if α_{e-v} were a composite quantity were considered by assuming that the exchange water in the system during experiments was a mixture of two phases, a gaseous phase and an adsorbed phase. Also, it is assumed that: (1) the D/H fractionation factor between adsorbed H_2O and water vapor mimics the liquid H_2O-vapor $^{D}\alpha_{L-V}$ value of 1.075 at 22 °C (e.g., Horita and Wesolowski, 1994); and (2) the D/H fractionation factor between HTN hydrogen and water vapor is ~0.996 as previously obtained by Yapp and Poths (1995). With these assumptions and the data on vapor fractions in Table 2, composite values of α_{e-v} for each of the samples can be calculated. Using these composite α_{e-v} values, the samples of groups 1, 2 and 3 collectively yield a regression slope for $1000\ln{}^{D}\alpha_{G-W}$ vs. X_{Al} of ~123, which is analytically indistinguishable from the values discussed previously. In contrast, results of this speculative procedure when applied to group 4 were anomalous. For example, the calculated $^{D}\alpha_{G-W}$ value for the Al-free sample (SFO-4-13) of group 4 was 0.888 (±0.005) which differs significantly from the aforementioned value of 0.905 (±0.004). The reasons for the apparently anomalous behavior of group 4 in this speculative calculation are not known, but the outcome of this exercise for the four groups taken as a whole is to suggest that the positive correlation between $1000\ln{}^{D}\alpha_{G-W}$ and X_{Al} determined originally for these synthesis experiments is robust and therefore has credibility. This affirms published results which indicate that an adjustment of measured goethite δD values for degree of Al substitution in natural samples is important for interpretations of the data.

4. CONCLUSIONS

A two-component model for hydrogen in "outgassed" synthetic goethite is affirmed in this study. The isotopically exchangeable (at ~22 °C) HTN hydrogen component in these samples seems to be adequately characterized by a fractionation factor (α_{e-v}) with respect to ambient exchange water of 0.942 (±0.02)for all of the synthetic goethites of this work. Using the nominal α_{e-v} value of 0.942, the D/H fractionation between structural hydrogen (in Al-free goethite) and ambient liquid water ($^{D}\alpha_{G-W}$) as determined for these synthetic goethites is ~0.900 (±0.006). This value is in agreement (within analytical uncertainty) with the published $^{D}\alpha_{G-W}$ value of 0.905 (±0.004) (Yapp, 1987).

For four groups of goethite syntheses, the magnitude of the effect of Al substitution on the value of $1000\ln{}^{D}\alpha_{G-W}$ is estimated to be 1.4 (±0.4)‰ per mol % Al. This effect does *not* appear to depend on pH of the syntheses over a range from ~1.5 to 14, nor does it depend on synthesis temperatures from 22 to 48 °C. This apparently linear dependence of $1000\ln{}^{D}\alpha_{G-W}$ on mol % of Al in goethite (over the observed range from 0 to 13 mol %) is consistent with the prediction of a thermodynamic mixing model (Yapp, 1993). However, the experimentally determined slope of 1.4 (±0.4)‰ per mol % Al is somewhat larger than the value of 0.7‰ per mol % Al determined using boehmite as the AlOOH endmember in the published model. The overall uncertainties in the current results of these difficult exchange experiments suggest that the approximation of an Al effect of ~1‰ per mol % Al may be a reasonable estimate with which to adjust δD values of natural goethites to those of the pure FeOOH endmember and could be valid for degrees of Al substitution of up to at least 15 mol %.

Yapp's model (1993) also predicted that oxygen isotopic fractionation between goethite and ambient water (expressed as $1000\ln{}^{18}\alpha_{G-W}$) should be a linear function of Al mole fraction. Further work is planned to test for this effect in synthetic goethite.

ACKNOWLEDGMENTS

This research was supported by NSF Grant EAR-0616627 to C.J. Yapp. The paper benefited from the helpful reviews of David Cole, Albert Gilg and two anonymous reviewers.

REFERENCES

Bao H. and Koch P. L. (1999) Oxygen isotopic fractionation in ferric oxide-water systems: low temperature synthesis. *Geochim. Cosmochim. Acta* **63**, 599–613.

Barrow G. M. (1966) *Physical Chemistry*, Second edition. McGraw-Hill, New York.

Boily J.-F., Szanyi J. and Felmy A. R. (2006) A combined FTIR and TPD study on the bulk and surface dehydroxylation and decarbonation of synthetic goethite. *Geochim. Cosmochim. Acta* **70**, 3613–3624.

Cornell R. M. and Giovanoli R. (1985) Effects of solution conditions on the proportion and morphology of goethite formed from ferrihydrite. *Clays Clay Min.* **33**, 424–432.

Cornell R. M., Giovanoli R. and Schindler P. W. (1987) Effects of silicate species on the transformation of ferrihydrite into goethite and hematite in alkaline media. *Clays Clay Min.* **35**, 12–28.

Cornell R. M. and Schwertmann U. (2003) *The iron oxides: Structure, Properties, Reactions, Occurrences and Uses*, Second edition. Wiley-WCH, Weinheim.

Craig H. (1961) Isotopic variations in meteoric waters. *Science* **133**, 1702–1703.

Davey B. G., Russell J. D. and Wilson M. J. (1975) Iron oxide and clay minerals and their relation to colours of red and yellow Podzolic soils near Sydney, Australia. *Geoderma* **14**, 125–138.

Girard J. P., Freyssinet P. and Chazot G. (2000) Unraveling climatic changes from intra-profile variation in oxygen and

hydrogen isotopic composition of goethite and kaolinite in laterites: an integrated study from Yaou, French Guiana. *Geochim. Cosmochim. Acta* **64**, 409–426.

Girard J. P., Freyssinet P. and Morillon A. C. (2002) Oxygen isotope study of Cayenne duricrust paleosurfaces: implications for past climate and laterization processes over French Guiana. *Chem. Geol.* **191**, 329–343.

Girard J. P., Razandranoroso D. and Freyssinet P. (1997) Laser oxygen isotope analysis of weathering goethite from the lateritic profile and Yaou, French Guiana: paleoweathering and paleoclimatic implications. *Appl. Geochem.* **12**, 163–174.

Glasauer S., Friedl J. and Schwertmann U. (1999) Properties of goethites prepared under acidic and basic conditions in the presence of silicate. *J. Colloid Interface Sci.* **216**, 106–115.

Gonfiantini R. (1978) Standards for stable isotope measurements in natural compounds. *Nature* **271**, 534–536.

Goodman B. A. and Lewis D. G. (1981) Mossbauer Spectra of aluminous goethite α-FeOOH. *J. Soil Sci.* **32**, 351–363.

Horita J. and Wesolowski D. J. (1994) Liquid–vapor fractionation of oxygen and hydrogen isotopes of water from the freezing to the critical temperature. *Geochim. Cosmochim. Acta* **59**, 3425–3437.

Hren M. T., Lowe D. R., Tice M. M., Byerly G. and Chamberlain C. P. (2006) Stable isotope and Rare Earth Element evidence for recent ironstone pods within the Archean Barberton greenstone belt, South Africa. *Geochim. Cosmochim. Acta* **70**, 1457–1470.

Hsieh Jean C. C. and Yapp C. J. (1999) Stable carbon isotope budget of CO_2 in a wet, modern soil as inferred from $Fe(CO_3)OH$ in pedogenic goethite; possible role of calcite dissolution. *Geochim. Cosmochim. Acta* **63**, 767–783.

Lewis D. G. and Schwertmann U. (1979) The influence of aluminum on the formation of iron oxides.. IV. The influence of [Al], [OH], and Temperature. *Clays Clay Min.* **27**, 195–200.

Mendelovici E., Yariv S. h. and Villalba R. (1979) Aluminum-bearing goethite in Venezuelan laterites. *Clays Clay Min.* **27**, 368–372.

Müller J. (1995) Oxygen isotopes in iron (III) oxides: a new preparation line; mineral–water fractionation factors and paleoenvironmental considerations. *Isot. Environ. Health Stud.* **31**, 301–302.

Norrish K. and Taylor R. M. (1961) The isomorphous replacement of iron by aluminum in soil goethites. *J. Soil Sci.* **12**, 294–306.

Powell R. (1978) *Equilibrium Thermodynamics in Petrology*. Harper & Row, London/New York.

Savin S. and Epstein S. (1970) The oxygen and hydrogen isotope geochemistry of clay minerals. *Geochim. Cosmochim. Acta.* **3**, 25–42.

Schulze D. G. (1984) The influence of aluminum on iron oxides. VIII. Unit-Cell dimensions of Al-substituted goethite and estimation of Al from them. *Clays Clay Min.* **32**, 36–44.

Schulze D. G. and Schwertmann U. (1984) The influence of aluminum on iron oxides: X. Properties of Al-substituted goethites. *Clay Min.* **19**, 512–539.

Schulze D. G. and Schwertmann U. (1987) The influence of aluminum on iron oxides: XIII. Properties of goethites synthesized in 0.3 M KOH at 25 °C. *Clay Min.* **22**, 83–92.

Schwertmann U. (1984) The influence of aluminum on iron oxides: IX. Dissolution of Al–goethite in 6 M HCl. *Clay Min.* **19**, 9–19.

Schwertmann U., Friedl J., Stanjek H. and Schulze D. G. (2000a) The effect of clay minerals on the formation of goethite and hematite from ferrihydrite after 16 years' ageing at 25 °C and pH 4–7. *Clay Min.* **35**, 613–623.

Schwertmann U., Friedl J., Stanjek H. and Schulze D. G. (2000b) The effect of Al on Fe oxides. XIX. Formation of Al-substituted hematite from ferrihydrite at 25 °C and pH 4–7. *Clays Clay Min.* **48**, 159–172.

Schwertmann U. and Murad E. (1983) Effect of pH on the Formation of Goethite and Hematite from Ferrihydrite. *Clays Clay Min.* **31**, 277–284.

Tabor N. J. (2007) Permo-Pennsylvanian palaeotemperatures from Fe-Oxide and phyllosilicate $\delta^{18}O$ values. *Earth Planet. Sci. Lett.* **253**, 159–171.

Tabor N. J. and Yapp C. J. (2005) Juxtaposed Permian and Pleistocene isotopic archives; surficial environments recorded in calcite and goethite from the Wichita Mountains, Oklahoma. In *Special Paper-Geological Society of America: Isotopic and Elemental Tracers of Cenozoic Climate Change*, vol. 395 (eds. G. Mora and D. Surge), pp. 55–70.

Tabor N. J., Yapp C. J. and Montanez I. P. (2004a) Goethite, calcite, and organic matter from Permian and Triassic soils; carbon isotopes and CO_2 concentrations. *Geochim. Cosmochim. Acta* **68**, 1503–1517.

Tabor N. J., Montanez I. P., Zierenberg R. and Currie BS. (2004b) Mineralogical and geochemical evolution of a basalt-hosted fossil soil (Late Triassic, Ischigualasto Formation, northwest Argentina); potential for paleoenvironmental reconstruction. *GSA Bull.* **116**, 1280–1293.

Xu B.-L., Zhou G.-T. and Zheng Y.-F. (2002) An experimental study of oxygen isotope fractionations in goethite–akaganeite–water systems at low temperature (in Chinese). *Geochimica* **31**, 366–374.

Yapp C. J. (1987a) A possible goethite–iron (III) carbonate solid solution and the determination of CO_2 partial pressure in low-temperature geological systems. *Chem. Geol.* **64**, 259–268.

Yapp C. J. (1987b) Oxygen and hydrogen isotope variations among goethites (α-FeOOH) and the determination of paleotemperatures. *Geochim. Cosmochim. Acta* **51**, 355–364.

Yapp C. J. (1990) Oxygen isotopes in iron (III) oxides. 1. Mineral–water fractionation factors. *Chem. Geol.* **85**, 329–335.

Yapp C. J. (1991) Oxygen isotope in an oolitic ironstone and the determination of goethite $\delta^{18}O$ values by selective dissolution of impurities: the 5 M NaOH method. *Geochim. Cosmochim. Acta* **55**, 2627–2634.

Yapp C. J. (1993) The stable isotope geochemistry of low temperature Fe(III) and Al oxides with implications for continental paleoclimates. In *Climate Change in Continental Isotopic Records*, vol. 78 (eds. P. K. Swart, K. C. Lohmann, J. A. McKenzie and S. Savin) Geophys. Monography, pp. 285–294.

Yapp C. J. (1997) An assessment of isotopic equilibrium in goethites from a bog iron deposit and a lateritic regolith. *Chem. Geol.* **135**, 159–171.

Yapp C. J. (1998) Paleoenviromental interpretation of oxygen isotope ratios in oolitic ironstones. *Geochim. Cosmochim. Acta* **62**, 2409–2420.

Yapp C. J. (2000) Climatic implications of surface domains in arrays of δD and $\delta^{18}O$ from hydroxyl minerals: goethite as an example. *Geochim. Cosmochim. Acta* **64**, 2009–2025.

Yapp C. J. (2001a) Rusty Relics of Earth History: iron (III) oxides, isotopes, and surficial environments. *Annu. Rev. Earth Planet Sci.* **29**, 165–199.

Yapp C. J. (2001b) Mixing of CO_2 in surficial environments as recorded by the concentration and $\delta^{13}C$ values of the $Fe(CO_3)OH$ component in goethite. *Geochim. Cosmochim. Acta* **65**, 4115–4130.

Yapp C. J. (2004) $Fe(CO_3)OH$ in goethite from a mid-latitude North American Oxisol: Estimate of atmospheric CO_2 concentration in the Early Eocene "Climatic optimum". *Geochim. Cosmochim. Acta* **68**, 935–947.

Yapp C. J. (2007) Oxygen isotopes in synthetic goethite and a model for the apparent pH dependence of goethite–water $^{18}O/^{16}O$ fractionation. *Geochim. Cosmochim. Acta* **71**, 1115–1129.

Yapp C. J. and Pedley M. D. (1985) Stable hydrogen isotopes in iron oxides: II, D/H variations among natural goethites. *Geochim. Cosmochim. Acta* **49**, 487–495.

Yapp C. J. and Poths H. (1992) Ancient atmospheric CO_2 pressure inferred from natural goethites. *Nature* **355**, 342–344.

Yapp C. J. and Poths H. (1993) The carbon isotope geochemistry of goethite (α-FeOOH) in ironstone of the Upper Ordovician Neda Formation, Wisconsin, USA: implications for early Paleozoic continental environments. *Geochim. Cosmochim. Acta* **57**, 2599–2611.

Yapp C. J. and Poths H. (1995) Stable hydrogen isotopes in iron oxides: III. Nonstoichiometric hydrogen in goethite. *Geochim. Cosmochim. Acta* **59**, 3405–3412.

Zheng Y.-F. (1998) Oxygen isotopic fractionation between hydroxide minerals and water. *Phys. Chem. Miner.* **25**, 213–221.

Associate editor: David R. Cole